

T. Tala, K.-D. Zastrow, J. Ferreira, P. Mantica, V. Naulin, A.G. Peeters, G. Tardini,
M. Brix, G. Corrigan, C. Giroud, D. Strintzi and JET EFDA contributors

Evidence of Inward Toroidal Momentum Convection in the JET Tokamak

"This document is intended for publication in the open literature. It is made available on the understanding that it may not be further circulated and extracts or references may not be published prior to publication of the original when applicable, or without the consent of the Publications Officer, EFDA, Culham Science Centre, Abingdon, Oxon, OX14 3DB, UK."

"Enquiries about Copyright and reproduction should be addressed to the Publications Officer, EFDA, Culham Science Centre, Abingdon, Oxon, OX14 3DB, UK."

Evidence of Inward Toroidal Momentum Convection in the JET Tokamak

T. Tala¹, K.-D. Zastrow², J. Ferreira³, P. Mantica⁴, V. Naulin⁵, A.G. Peeters⁶, G. Tardini⁷,
M. Brix², G. Corrigan², C. Giroud², D. Srintzi⁸ and JET EFDA contributors*

JET-EFDA, Culham Science Centre, OX14 3DB, Abingdon, UK

¹*Association EURATOM-Tekes, VTT, P.O. Box 1000, FIN-02044 VTT, Finland*

²*EURATOM-UKAEA Fusion Association, Culham Science Centre, OX14 3DB, Abingdon, OXON, UK*

³*Associação EURATOM/IST, Instituto de Plasmas e Fusão Nuclear, 1049-001 Lisbon, Portugal*

⁴*Istituto di Fisica del Plasma CNR-EURATOM, via Cozzi 53, 20125 Milano, Italy*

⁵*Association Euratom-Risø DTU, DK-4000 Roskilde, Denmark*

⁶*Center for Fusion, Space and Astrophysics, Department of Physics, University of Warwick, CV4 7AL, UK*

⁷*Max-Planck-Institut für Plasmaphysik, EURATOM-Assoziation, D-85748, Garching, Germany*

⁸*National Technical University of Athens, Euratom Association, GR-15773 Athens, Greece*

** See annex of M.L. Watkins et al, "Overview of JET Results",
(Proc. 21st IAEA Fusion Energy Conference, Chengdu, China (2006)).*

ABSTRACT.

Experiments have been carried out on the Joint European Torus (JET) tokamak to determine the diffusive and convective momentum transport. Torque, injected by neutral beams, was modulated to create a periodic perturbation in the toroidal rotation velocity. Novel transport analysis shows the magnitude and profile shape of the momentum diffusivity is similar to those of the ion heat diffusivity. A significant inward momentum pinch, up to 20 m/s, has been found. Both results are consistent with recent developments in momentum transport theory and gyro-kinetic simulations. This evidence is complemented in plasmas with internal transport barriers.

INTRODUCTION

Plasma rotation and momentum transport in tokamaks are currently a very active research area. It is well-known that sheared rotation can lead to quenching of turbulence and a subsequent improvement in confinement [1,2]. Toroidal rotation also increases stability against pressure limiting resistive wall modes [3]. Still, transport of toroidal momentum is less understood than heat or particle transport. Extrapolating reliably the toroidal rotation, in magnitude and profile shape to future tokamaks, such as ITER, remains a challenge, as neither momentum transport nor sources are known precisely. One way to increase the understanding of momentum transport is to compare it with heat transport as for the conditions where the Ion Temperature Gradient (ITG) instability is dominantly driving anomalous transport, both transport channels are predicted to be similar [4,5]. The momentum diffusivity χ_ϕ and pinch velocity v_{pinch} are related to the toroidal velocity v_f , its gradient “ v_f and the momentum flux Γ_ϕ , assuming the absence of a significant particle flux, as follows:

$$G_\phi \sim -\chi_\phi \nabla(v_\phi n) - v_{pinch} v_\phi n = -\chi_{\phi,eff} \nabla(v_\phi n), \quad (1)$$

where n is the ion density. It is always possible to combine the diffusive and convective part of the momentum flux into an effective momentum diffusivity $\chi_{\phi,eff}$. This quantity can be easily determined from steady-state transport analysis once the sources are known while the determination of χ_ϕ and v_{pinch} separately requires more sophisticated experiments.

A rotation database covering more than 600 JET discharges shows that the effective Prandtl number, $P_{r,eff} = \chi_{\phi,eff}/\chi_{i,eff} \approx 0.1-0.4$ is substantially below one in the JET core plasma [6,7]. Somewhat larger values for $P_{r,eff}$ have been reported on other tokamaks [8,9]. The low $P_{r,eff}$ is in apparent contradiction with ITG based theories and gyro-kinetic calculations, which report ‘purely diffusive’ Prandtl number $P_r = \chi_\phi/\chi_i \approx 1$, with only weak dependencies on plasma parameters, like q , magnetic shear or density and temperature gradient [5,10]. Recent developments in theory predict a sizeable inward momentum pinch. This could resolve the discrepancy as the inward pinch results in $P_{r,eff}$ being smaller than P_r [11,12]. Until now experimental evidence for an inward momentum pinch has only been reported on the JT-60U tokamak [13]. In this Letter, we present experimental evidence of a significant inward momentum pinch in JET, using torque modulation techniques. This evidence

is complemented with observations in plasmas with Internal Transport Barriers (ITBs) showing different dynamic behaviour between ion temperature and toroidal velocity.

Studying heat transport by modulation of localised, electron or ion cyclotron resonance heating is a well established technique [14]. For momentum, the only significant torque source which can be modulated originates from the Neutral Beam Injection (NBI) system. Passing ions transfer toroidal angular momentum to the bulk plasma by collisions which is a slow process, whereas trapped ions transfer their momentum by $\mathbf{j} \times \mathbf{B}$ forces which is practically instantaneous (\mathbf{j} denotes displacement current density due to finite banana orbit width and \mathbf{B} magnetic field) [15].

An experiment where the NBI power and torque were modulated at 6.25 Hz has been performed on JET. This modulation frequency is much lower than the 10ms time resolution of the Charge Exchange Recombination Spectroscopy (CXRS) diagnostic used to measure the toroidal rotation ω_ϕ and ion temperature T_i at 12 radial points [16]. The modulation took place between $t=4$ s and $t=13$ s, using 3 tangential beams for a total of about 5 MW of modulated power. Time traces of experimental toroidal angular rotation frequency ω_ϕ and calculated torque for 9 of the modulation cycles are illustrated in figure 1(a) and (b), showing a clear modulation in ω_ϕ .

To perform the cleanest possible toroidal rotation modulation and to avoid MHD modes, a H -mode plasma with type III ELMs, low collisionality and high q_{95} was chosen. Under these conditions, ITG is the dominant instability, making the coupling of momentum and ion heat transport, and thus the concept of the Prandtl number, unambiguous.

The NBI induced torque has been calculated with the NUBEAM code [17] inside the TRANSP transport code. To obtain a torque modulation signal far beyond noise, 160 000 particles have been used in the Monte-Carlo calculation of NBI torque. All phases are calculated with reference to the phase of the NBI power. The calculated amplitude and phase at 6.25Hz of the modulated torque density profiles are shown in figure 1(c) as a function of the normalised toroidal flux co-ordinate. Outside $\rho > 0.4$ the torque is dominated by the $\mathbf{j} \times \mathbf{B}$ component and synchronous with the injected power while in the central part of the plasma, the collisional component dominates, resulting in a delay of about 50ms due to the slowing down time of the fast ionised beam particles. As the modulated torque is not radially localised, a simple determination of the momentum diffusivity and pinch directly from the spatial derivatives of the amplitude and phase of the modulated ω_ϕ is not viable. Therefore, time-dependent transport modelling of ω_ϕ is required.

The novel transport modelling methodology adopted in this study to determine the momentum diffusivity and pinch uses the following 3 steps: step 1, calculate $\chi_{i,\text{eff}}$; step 2, vary the P_r value and its radial profile to fit the simulated phase of the modulated rotation to the experimental phase profile, as the phase is not very sensitive to v_{pinch} ; step 3, vary v_{pinch} to best fit also the simulated amplitude of the modulated toroidal rotation to the experimental data, simultaneously also matching the steady-state. In step 1 $\chi_{i,\text{eff}}$ is calculated from the measured T_i data and calculated power deposition profiles. Step 2 leads to a rather precise identification of the acceptable range of P_r values, since P_r is the only unknown (the sources are taken from the NUBEAM calculations). This resolves the

indeterminacy associated with the analysis of only the steady-state profile, as the latter can be reproduced by an unlimited number of possible combinations for χ_ϕ and v_{pinch} yielding the same $\chi_{\phi,\text{eff}}$. Once P_r is identified, step 3 allows us to identify v_{pinch} needed to reproduce the steady-state ω_ϕ and amplitude with the chosen P_r value. As a refinement, P_r , instead of being constant, can be chosen to have a radial profile, taken e.g. from gyro-kinetic simulations.

Figures 2-3 compare experimental data and simulations for ω_ϕ steady-state and modulated amplitude $A_{\omega,\phi}$ and phase $\varphi_{\omega,\phi}$. The experimental profiles have been mapped onto a moving equilibrium to eliminate the spurious modulation components due to modulated plasma position. For the simulations, the two most obvious options for \llcorner_f or P_r and v_{pinch} were adopted: (i) fix $P_r=0.25$ to yield $\chi_\phi = 0.25\chi_{i,\text{eff}}$ and $v_{\text{pinch}}=0$ or (ii) match the simulated and experimental phase by fitting P_r , using the profile shape from gyro-kinetic simulations with GKW [18] and then vary the v_{pinch} profile to additionally match the simulated and experimental amplitudes and steady-state. All simulations for ω_ϕ have been performed with the JETTO transport code. The transport equation for ω_ϕ is solved while q , T_i , T_e and n_e are frozen to their experimental values. The boundary conditions for steady-state ω_ϕ and the amplitudes $A_{\omega,\phi}$ and phases $\varphi_{\omega,\phi}$ of the modulated ω_ϕ are chosen to fit the experimental data at $\rho=0.8$. The transport simulations are carried out over the 9 modulation cycles shown in figure 1.

Both simulations (i) and (ii) predict the steady-state ω_ϕ within 10% accuracy in the region of interest, i.e. $0.2 < \rho < 0.8$, as seen in figure 2. Inside $\rho < 0.2$, neo-classical transport starts to dominate ion heat transport, and the predictions are worse as the use of the ITG based P_r for calculating \llcorner_f is not appropriate.

Options (i) and (ii) differ, however, in reproducing the $A_{\omega,\phi}$ and ω_ϕ profiles as shown in figure 3. Case (i) with $P_r = 0.25$ and $v_{\text{pinch}} = 0$ clearly disagrees with the experiments. The simulated phase is too large, an indication of too low χ_ϕ , i.e. too low P_r used in the simulation. On the other hand, the simulated amplitude is too low towards the plasma centre, which could only be cured by lowering χ_ϕ further. This shows that the assumption $v_{\text{pinch}} = 0$ is not compatible with the experimental data. Case (ii) uses $P_r = \chi_\phi/\chi_i \sim 1$ from GKW (figure 4(c)) and v_{pinch} varying radially between 0 and 25 m/s (figure 4(d)). This improves the agreement between the simulated and experimental amplitudes and phases dramatically. The $\chi_{i,\text{eff}}$ used as χ_i (heat pinch assumed to be zero) to multiply P_r , is also shown in figure 4(d). This v_{pinch} profile reproduces best the experimental amplitude and phase profiles, together with an acceptable reproduction of the steady-state toroidal rotation profile. v_{pinch} is roughly proportional to χ_ϕ , consistent with the predictions by the theory [11,12]. Uniform $P_r=1.0$ instead of using P_r from GKW and the same v_{pinch} results in almost as good agreement with experiment. Finally, while the P_r numbers from GKW used in the JETTO simulations are in excellent agreement with experiment, and also very similar to those calculated with GS2 [19], there is some discrepancy in the pinch numbers, defined as $Rv_{\text{pinch}}/\chi_\phi$. The pinch numbers from GKW are 2–4, depending on radius, whereas the experimental ones are in the range of 3–8.

A sensitivity analysis shows that 20–30% variability in P_r and v_{pinch} is compatible with

experimental data, while outside this range the simulated phase and amplitude deviate unacceptably from the experimental values. The TRANSP torque calculations have been found very robust with respect to variations in plasma parameters.

One complicating factor requiring a careful assessment is that the ion and electron temperatures are also modulated with peak amplitudes around 70eV, i.e. a perturbation of just below 1% to be compared with the amplitude of the ω_ϕ modulation being around 4%. A time variation of T_i and/or its gradient length induces a time variation in the ITG driven transport, causing an oscillation in χ_i . This leads to an oscillation in χ_ϕ , yielding an extra contribution to A_{ω_ϕ} and φ_{ω_ϕ} and possibly modifying the determined P_r and v_{pinch} . To estimate the impact of such T_i modulation on the determined P_r and v_{pinch} , a time-dependent χ_i using an ion heat transport model based on the critical gradient length concept [20] and with the typical ion heat transport parameters found in JET ion heat transport studies [21], has been used to model the modulated T_i and the associated time variation of χ_i and χ . Owing to the small amplitude of the T_i modulation, the effect on the values determined for P_r and v_{pinch} was insignificant.

Further, additional evidence of the existence of inward momentum pinch on JET comes from a plasma with an ITB. It has been reported that the footpoint of the ITB coincides between all transport channels (T_i , T_e , n_e , ω_ϕ) and that the radial expansion of the ITB occurs simultaneously for all channels [22]. The present experimental observation, however, illustrates that the footpoint of the ITB seems to be located at a slightly larger radius in T_i than in ω_ϕ as the ITB moves radially outwards. In figure 4, the T_i barrier is located within the CXRS channel (marked as horizontal lines in frame (d)) centred at $r/a=0.48$ whereas the ω_ϕ barrier is located one CXRS channel more inwards, i.e. centred at $r/a=0.41$ at $t=5.29-5.31$ s. This can be seen clearly in frames (c) and (d) where there is virtually no difference in $\Delta\omega_\phi$ (between blue (dotted) and magenta (plusses) curves) while there is a significant difference in ΔT_i at $r/a=0.48$. At $t=5.35$ s, the ω_ϕ barrier also appears at $r/a=0.48$ (black stars). The ITB moves steadily outwards, following the outward movement of the q_{min} surface, the footpoint reaching a radius $r/a=0.65$ until the ITB collapses at $t=5.95$ s. During its radial outward movement, the ITB passes two other CXRS channels at $r/a=0.58$ at $t=5.34$ s and $r/a=0.66$ at $t=5.77$ s. Both times, the ITB is seen first in T_i and after a few tens of milliseconds in ω_ϕ , indicating that the footpoint of the ITB is indeed located at a more outward radius for T_i than for ω_ϕ . The actual distance between the footpoints of the ITB in T_i and ω_ϕ is, however, much less than the distance between two CXRS channels. This phenomenon is only seen during the fast expansion of the ITB and never with stationary or slowly moving ITBs.

In order to understand this observation, two hypotheses have been tested: (1) in the absence of v_{pinch} , ω_ϕ could respond more slowly than T_i to the turbulence suppression within the ITB as $\langle\langle_{i,\text{eff}}$ is larger than $\omega_\phi = \omega_{\phi,\text{eff}}$, i.e. $P_{r,\text{eff}}=0.3$ for this discharge and (2) an inward toroidal momentum pinch causes an apparent delay to the outward movement of the ITB in the ω_ϕ channel, combined with higher $\langle\langle_f$ yielding P_r^a1 . To study these hypotheses, predictive transport simulations for T_i and ω_ϕ have been performed, with initial conditions for T_i and ω_ϕ taken from Pulse No. 69670. After

reaching steady-state, the radial outward movement of the ITB in the ion heat transport channel is simulated by moving the low χ_i region outwards with time. For momentum transport, the two options (1) and (2) are applied. In the simulation with $P_{r,eff} = 0.3$ and $v_{pinch} = 0$, T_i and ω_ϕ react to the change of χ_i in the same way, resulting in the footpoint of the ITB being exactly the same. In case (2), the v_{pinch} profile is assumed to be proportional to χ_i and normalised to the value consistent with the value found in the NBI modulation experiment ($v_{pinch} \sim 15$ m/s outside the ITB). This simulation shows that ω_ϕ responds more slowly to the radial outward movement of the ITB than T_i at the location of the ITB, as seen in figure 5. This is consistent with the CXRS measurements showing the rise of T_i just before the rise of ω_ϕ when the ITB passes the CXRS channel during its radial outward movement. It is to be noted that simulation (2) is sensitive to the v_{pinch} radial profile, which, in the absence of NBI modulation, cannot be determined. Here, we have assumed that inside the ITB, the magnitude of v_{pinch} is linked to the level of turbulence suppression, i.e. $v_{pinch} \sim \chi_i$.

CONCLUSIONS

In summary, consistent evidence for a significant inward momentum pinch has been found in JET. This may have important implications on the predictions for the toroidal velocity profile in ITER. In particular, a centrally peaked toroidal velocity profile may still result even in the absence of any external core momentum source. It still remains to be assessed if the parametric dependences of such a pinch term are such that a sizeable convective component will be present in ITER plasmas.

ACKNOWLEDGEMENTS

This work, supported by the European Communities under the contract of Association between EURATOM and Tekes, was carried out within the framework of the European Fusion Development. The views and opinions expressed herein do not necessarily reflect those of the European Commission.

REFERENCES

- [1]. Biglari H. *et al.*, Phys. Fluids B **2**, 1 (1990).
- [2]. Burrell K.H., Phys. Plasmas **4**, 1499 (1997).
- [3]. Garofalo A.M. *et al.*, Nucl. Fusion **41**, 1171 (2001).
- [4]. Mattor N. *et al.*, Phys. Fluids **31**, 1180 (1988).
- [5]. Peeters A.G. *et al.*, Phys. Plasmas **12**, 072515 (2005).
- [6]. de Vries P.C. *et al.*, Plasma Phys. Control. Fusion **48**, 1693 (2006).
- [7]. Tala T. *et al.*, Plasma Phys. Control. Fusion **49**, B291 (2007).
- [8]. Nishijima D. *et al.*, Plasma Phys. Control. Fusion **47**, 89 (2005).
- [9]. de Grassie J.S. *et al.*, Nucl. Fusion **43**, 142 (2003).
- [10]. Strintzi D. *et al.*, Phys. Plasmas **15**, 044502 (2008).
- [11]. Peeters A.G. *et al.*, Phys. Rev. Lett. **98**, 265003 (2007).

- [12]. Hahm T.S. *et al.*, Phys. of Plasmas **14**, 072302 (2007).
 [13]. Yoshida M. *et al.*, Nucl. Fusion **47**, 856 (2007).
 [14]. Lopez Carzodo N. J., Plasma Phys. Control. Fusion **37**, 799 (1995).
 [15]. Zastrow K.-D. *et al.*, Nuclear Fusion **38**, 257 (1998).
 [16]. Negus C.R. *et al.*, Rev. Sci. Instr. **77**, 10F102 (2006).
 [17]. Pankin A. *et al.*, Computer Physics Communications **159**, 157 (2004).
 [18]. Peeters A.G. *et al.*, Phys. Plasmas **11**, 3748 (2004).
 [19]. Kotschenreuther M. *et al.*, Computational Phys. Communication **88**, 128 (1995).
 [20]. Garbet X. *et al.*, Plasma Phys. Control. Fusion **46**, 1351 (2004).
 [21]. Ryter F. *et al.*, “Simultaneous Analysis of Ion and Electron Heat Transport by Power Modulation in JET”, submitted to IAEA FEC (2008).
 [22]. Challis C.D *et al.*, Plasma Phys. Control. Fusion **44**, 1031 (2002).

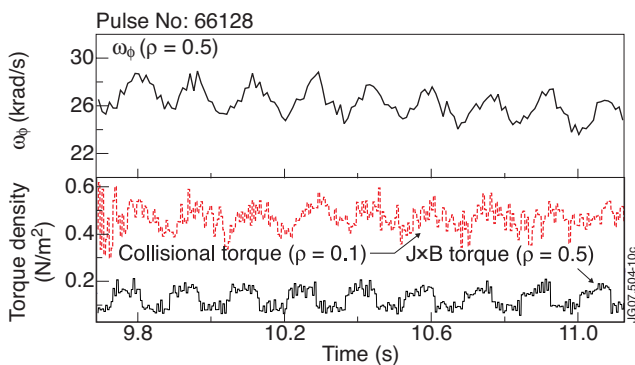


Figure 1: Time traces of (a) toroidal angular frequency ω_ϕ and (b) two components of the torque density for JET Pulse No. 66128. (c) Amplitude (solid black) and phase (dashed red) of the modulated calculated total torque.

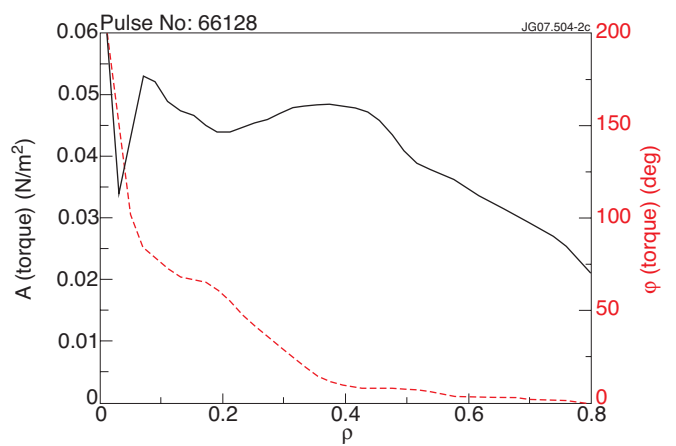


Figure 2: The simulated steady-state ω_ϕ with the two options (i) (dotted blue) and (ii) (dashed red) compared with the experimental ω_ϕ (solid black) with error bars.

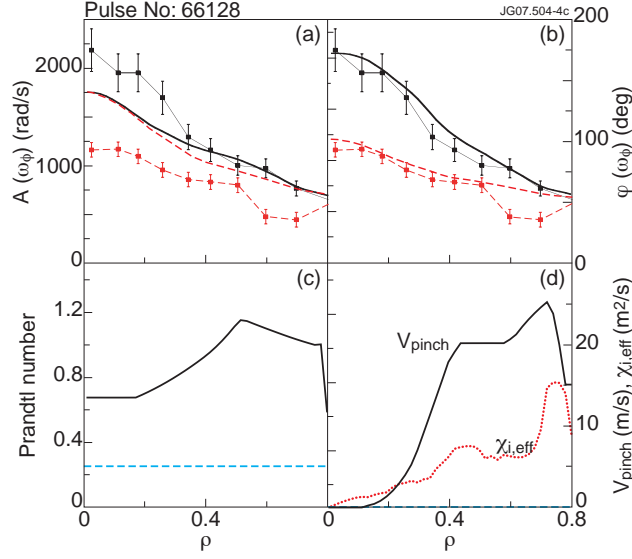


Figure 3: Comparison of the experimental amplitude (black solid with error bars) and phase (red dashed with error bars) and simulated amplitudes $A_{\omega,\phi}$ (black solid) and phases $j_{\omega,\phi}$ (red dashed) of modulated ω_ϕ with the simulation choice (i) in frame (a) and choice (ii) in frame (b). (c) Prandtl numbers and (d) pinch velocity profiles used in simulations (i) (blue dashed) and (ii) (black solid). Also shown the used $\chi_{i,eff}$ (red dotted) in frame (d).

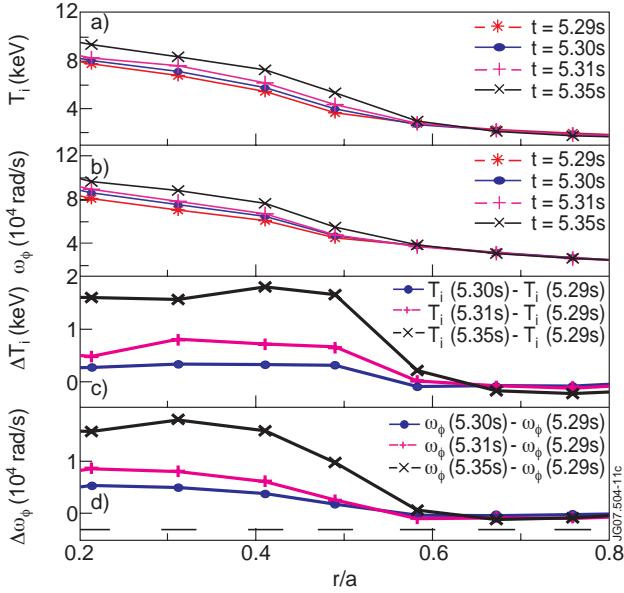


Figure 4: (a) T_i , (b) ω_ϕ , (c) ΔT_i and (d) $\Delta\omega_\phi$ profiles for JET Pulse No: 69670 during the radial expansion of the ITB. The horizontal lines shown in frame (d) indicate the radial widths of the CXRS measurements points.

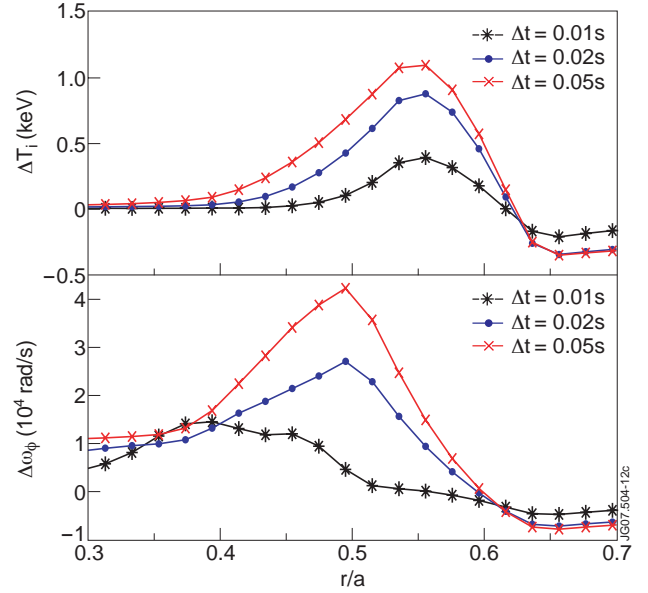


Figure 5: As in figure 5, but for simulated (a) ΔT_i and (b) $\Delta\omega_\phi$ profiles with a model of $v_{pinch} \sim 15m/s$ and $P_r = 1.0$.